Biolog. J. Armenia, *Special issue: Cyclodextrins*, 2001

CURRENT STATUS OF ATP-ase PROTON PUMP INHIBITOR COMPLEXATION WITH CYCLODEXTRINS

L. Marzocchi[*], J.R. Moyano[**], A. Rossi[*], P. Muñoz[**], M.J. Arias[**], F. Giordano[*]

[*] *Department of Pharmacy, Faculty of Pharmacy, University of Parma, Viale delle Scienze 27A, 43100 Parma, Italy.*

[**] *Department of Pharmacy and Pharmaceutical Technology, Faculty of Pharmacy, University of Seville, C./ Profesor García Gonzalez s/n. 41012 Seville, Spain.*

The inclusion complexes of cyclodextrins with drugs where the changes brought to the physical, chemical and biological properties of the guest molecules endow the final product with considerable pharmaceutical potential. The complexation properties of β- and γ-cyclodextrins with a variety of drugs widely used in clinical practice such as omeprazole and gliclazide have been studied. The researches on the interactions between cyclodextrins and a particular class of drugs known as the proton pump inhibitors have been carried out.

Инклюзионные комплексы циклодекстринов с лекарствами, которые приводят к изменениям физических, химических и биологических особенностей молекул "гостя", наделяют конечный продукт определенным фармацевтическим потенциалом. Изучены свойства комлесообразования β- и γ-циклодекстринов с разными лекарствами, широко используемыми в клинической практике, как омепразол и гликлазид. Проведены исследования по изучению взаимолействия между циклодекстринами и особым классом лекарств, известных как ингибиторы протонового насоса.

Ցիկլոդեքստրինների և դեղերի ինկլյուզիոն համալիրները, որոնք բերում են «հյուրի» մոլեկուլների ֆիզիկական, քիմիական և կենսաբանական առանձնահատկությունների փոփոխություններին, օժտում են վերջնական նյութը որոշակի դեղագործական պոտենցիալով: Ուսումնասիրվել են β և γ-ցիկլոդեքստրինների հետ տարբեր դեղերի, ինչպես կլինիկայում լայնորեն կիրառվող օմեպրազոլի և գլիկլազիդի, համալիրագոյացման հատկությունները: Ուսումնասիրվել են դեղերի հատուկ խմբի, որոնք հայտնի են որպես պրոտոնային մխոցի արգելակիչներ, և ցիկլոդեքստրինների միջև փոխազդեցությունները:

Introduction

Cyclodextrins have come a long way since they were first isolated by Villiers in 1891 from the degradation products of starch in butyric fermentation [1] and since their preparation and complete characterization by Schardinger in the early 1900s [2]. Their ability to form inclusion compounds as a result of host-guest complexation, both in the solid state and in solution, is widely appreciated in various sectors [3] and particularly, of direct interest to us, in the field of Pharmaceutical Development [4].

Cyclodextrins are cyclic (α–1,4)–linked oligosaccharides of α–D–glucopyranose which, owing to the impossibility of free rotation about the connecting glycosidic bonds, assume the shape of a torus or a truncated cone rather than that of a perfectly cylindrical molecule (Figure 1). The carbon skeleton of each glucose monomer, present in a $^1C_4$ chair conformation, together with the interconnecting ether bridges delimit an interior, hydrophobic cavity whereas all the hydroxyl groups are oriented outwards to form a hydrophilic external surface. The primary hydroxyl groups are orientated in such a way as to

form the narrow rim of the torus while the secondary hydroxyl groups define the wider rim [5]. The most common cyclodextrins, α-, β- and γ-, are made up of six, seven and eight glucopyranose units respectively. One can easily imagine the central cavity housing hydrophobic/lipophilic, and hence poorly hydrosoluble substances, engulfing them in a hydrophilic shield. Indeed, this is what happens during the formation of inclusion compounds where the changes brought to the physical, chemical and biological properties of the guest molecules endow the resulting complex with considerable pharmaceutical potential [6].

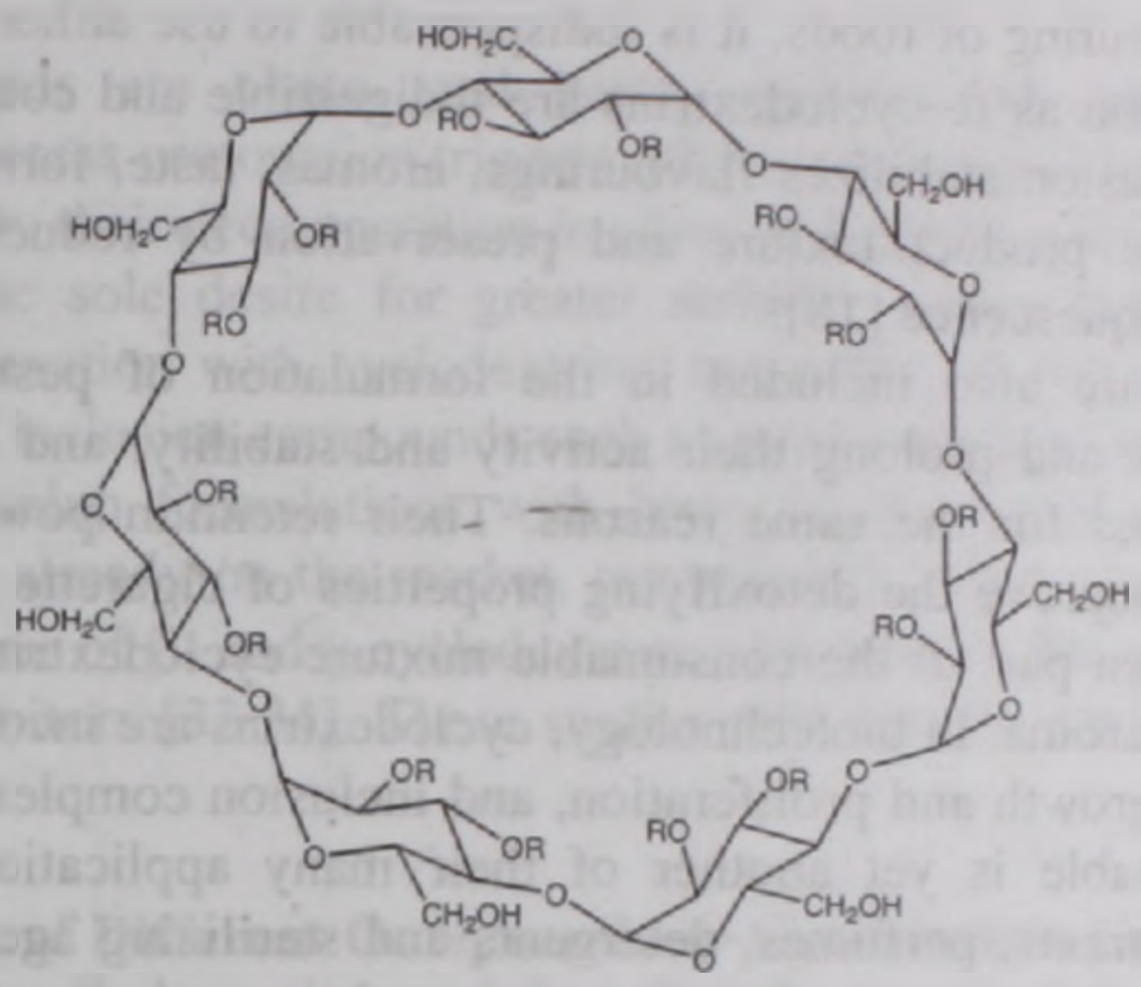

Figure 1. Molecular Structure of β-CD (R=H).

The formation of such inclusion complexes does not involve the formation of covalent bonds and, in aqueous solution, drug molecules are in dynamic equilibrium with those held within the cyclodextrin cavity. The main driving force of complex formation is probably the release of enthalpy-rich water molecules located inside the cavity that cannot satisfy their hydrogen bond potential and are of a higher enthalpy than the water molecules in solution [7, 8]. During complexation, the binding of non-polar drug molecules releases enthalpy-rich water molecules from the cavity into solution and the energy of the system is lowered [9].

Cyclodextrins occupy an important and ever-expanding pharmaceutical niche [10]. They are put to use essentially to increase molecular stability, enhance drug solubility in aqueous solutions, improve dissolution rate and bioavailability [11-13]. Other uses include that of converting liquid drugs into microcrystalline powders, preventing drug-drug or drug-excipient interactions, reducing drug irritation after oral or topical administration and improving the organoleptic characteristics of the formulation. Stability improvement aims at decreasing volatility and bettering heat stability, resistance to oxidation and hydrolysis whereas, improved drug-bioavailability from a cyclodextrin-containing formulation arises predominantly from an increase in the apparent solubility of the hydrophobic drug which would normally be prone to a dissolution rate-limited absorption.

Indeed, such interactions have been studied extensively and several inclusion complexes are now on the market in Japan and Europe [14]. In the U.S.A., cyclodextrin-containing products have not yet met with F.D.A. approval which is unfortunate because such an approval conditions worldwide opinion and would be of paramount importance to pharmaceutical use and commercial viability of these valuable materials [15].

Furthermore, cyclodextrins and their derivatives have found their way into countless products of the cosmetic, chemical and alimentary industries where inclusion compounds continue to be appreciated for their enhanced solubility of poorly hydrosoluble compounds and their molecular stabilization to heat, oxidation, light and hydrolysis [16].

In cosmetics, β–cyclodextrin inclusion compounds are used as an alternative method to the micellar solubilization of liposoluble ingredients which usually employs potentially irritating surfactants, for their slow and prolonged release of colorants and perfumes, for stabilizing essential oils and protecting them from oxidation and volatilization and for their ability to include malodorous compounds [17].

In the manufacturing of foods, it is indispensable to use either β– or γ–cyclodextrins for human consumption as α–cyclodextrins are indigestible and could lead to problems of chronic toxicity. Inclusion stabilizes flavourings, aromas, taste, form and colour, and may also help to improve product texture and preservation by reducing the end product's hygroscopicity or deliquescence [18].

Cyclodextrins are also included in the formulation of pesticides, herbicides and fungicides to enhance and prolong their activity and stability, and in products containing plant growth hormones for the same reasons. Their retention power is exploited by the tobacco industry to improve the detoxifying properties of cigarette filters against nicotine and tars whereas, when part of the consumable mixture cyclodextrins are used to stabilize and enhance tobacco aroma. In biotechnology, cyclodextrins are incorporated in cell culture media to favour cell growth and proliferation, and inclusion complexation with enzymes to render them more stable is yet another of their many applications. Anti-foam agents, industrial dyes, deodorants, perfumes, detergents and sterilizing agents are only but a few other examples from the never ending list of countless cyclodextrin-containing products [19].

Of equal importance is the application of natural and modified cyclodextrins in the field of analytical chemistry. Here, they have been successfully employed in chiral capillary electrophoresis [20] as the chiral selector component of the background electrolytes [21], as chiral stationary phases in both liquid and gas chromatography and as selective components of the mobile phase in thin layer and high performance liquid chromatography [22]. The basis of this use lies in the ability of cyclodextrins to select guest molecules in view of their size and geometry.

Our research group has been working with cyclodextrins for some time now and in particular we have studied the complexation properties of β- and γ-cyclodextrins with a variety of drugs widely used in clinical practice such as omeprazole and gliclazide [23-26]. Here, we present a brief over-view of the research carried out on the interactions between cyclodextrins and a particular class of drugs known as the proton pump inhibitors.

H^+/K^+ ATP-ase Proton Pump Inhibitors.

The ultimate mediator of acid secretion in the stomach is the H^+/K^+ ATP-ase transmembranal protein uniquely present in the apical membrane of the parietal cell and commonly referred to as the proton pump. By covalently binding to certain critical cystein residues present in the extracellular luminal domain of this protein, the proton pump inhibitors block the conformational reassessments that are responsible for this protein's pumping action, and thus inhibit the extrusion of protons into the lumen of the stomach. In doing so, these drugs block both basal and stimulated secretion of gastric acid [27-29].

Omeprazole, Pantoprazole, Lansoprazole, Rabeprazole and now also Esomeprazole, which constitute this class of highly specific proton pump inhibitors, incorporate both a

benzimidazole moiety and a pyridine ring bridged together by a methylsulfinyl link (Figure 2). Theoretically, both of these aromatic portions are able to interact with the cyclodextrin cavity. At neutral pH these compounds are devoid of inhibitory activity and require an acidic environment for their activation and as such, these drugs are, in fact, prodrugs. On reaching the parietal cells from the blood, these neutral amphiphilic compounds diffuse into the secretory canaliculi where they become protonated and trapped, unable to cross back over the cellular membrane into the parietal cell. The protonated form rearranges to form a sulfenic acid and a sulfenamide and it is as a sulfenamide that these compounds form disulphides with the sulphydryl groups of the cysteinic amino acids to block the pump [30,31].

These compounds are photo- and heat- sensitive and cannot withstand acidic conditions. Infact, whereas protonation triggers off their biological activity *in vivo*, the same series of events leads to their decomposition *in vitro*, making them difficult to manage during drug formulation. The sole desire for greater stability makes these compounds perfect candidates for complexation with cyclodextrins, but other advantages may also be drawn from the formation of inclusion compounds such as greater aqueous solubility.

In order to develop formulations with better technological and biopharmaceutical properties than those already on the market, our research group carried out studies on the complexation behaviour of β- and γ-cyclodextrins with omeprazole, as the representative of the proton pump inhibitors [32-34]. These studies will now be dealt with in the following sections.

Thermal Study of Different Omeprazole–γ–Cyclodextrin Co-Ground Systems.

This first line of research employed techniques of thermal analysis, such as Differential Scanning Calorimetry (DSC), Thermal Gravimetric/Differential Thermal Gravimetric Analysis (TG/DTG), Evolved Gas Detection (EGD) and Hot Stage Microscopy (HSM) to study and characterize both the inclusion complexes formed and the state of dispersion obtained after co-grinding equimolar mixtures of omeprazole and γ-cyclodextrins under various conditions [32]. These techniques prove ideal for following inclusion complex formation, as they provide a precise insight into the binding events which occur between the cyclodextrin host and the guest molecules.

The samples were prepared by milling a 1:1 physical mixture of omeprazole (OME) and γ-cyclodextrin (γ-CD) in a semi industrial mill (Fritsch Pulverisette, type 02102) for 4 h following four different methods:

1. dry co-grinding;
2. wetting of physical mixture with absolute alcohol;
3. wetting of physical mixture with a 1:1 ethanol/phosphate buffer solution;
4. wetting of physical mixture with a phosphate buffer.

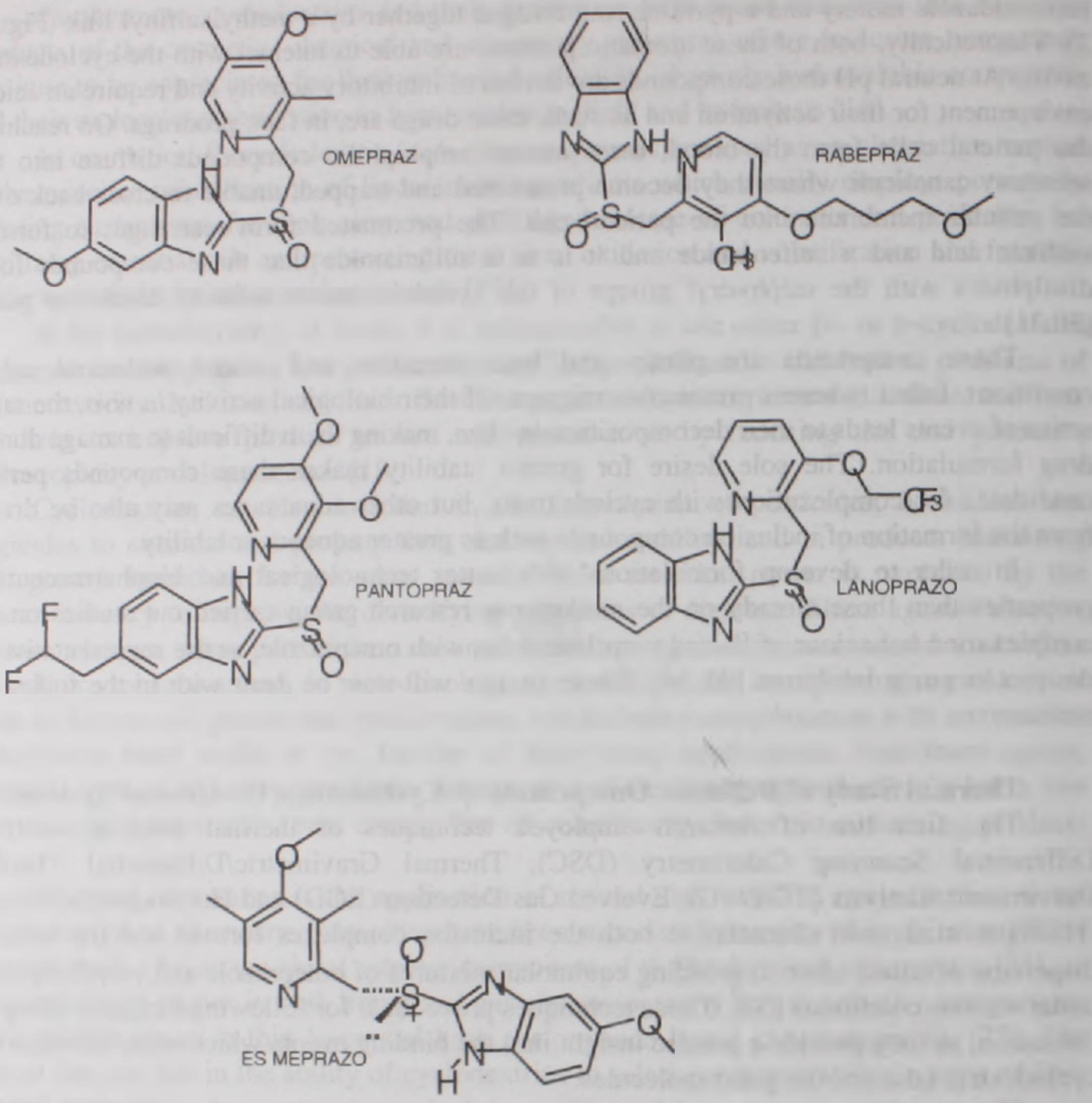

Figure 2. Molecular Structure of the Proton Pump Inhibitors.

The phosphate buffer was used instead of water to wet the systems in order to preserve the drug, under examination, from degradation.

The DSC curves of the co-ground systems were compared with those of the pure components, the dry-ground OME and the physical mixture (Figure 3). Curves 3(a) and 3(b) belong to OME and γ-CD respectively. Curve 3(a) is characterized by the presence of a sharp endothermic effect at 148°C due to fusion, followed by a broad exothermic peak at about 160°C caused by decomposition. In curve 3(b), two endothermic effects (a broad peak at 50°C and a less pronounced one at about 100°C) can be observed as a result of the gradual loss of two types of differently retained water molecules from pure γ-CD. Another endothermic peak at around 275°C indicates the onset of the solid's decomposition which is extended to the liquid phase after all the γ-CD has melted. Curve 3(c), arising from the physical mixture OME/γ-CD, is a mere superposition of the curves given by the pure components of the mixture, apart from dehydration occurring at a lower temperature.

indicating a tendency of the drug to favour CD dehydration [35]. From the DSC curve relative to dry-ground OME (curve 3(d)), it can be noted that the melting endotherm at about 150°C is less pronounced than that in curve 3(a), evidencing only partial amorphization of the drug during dry-grinding.

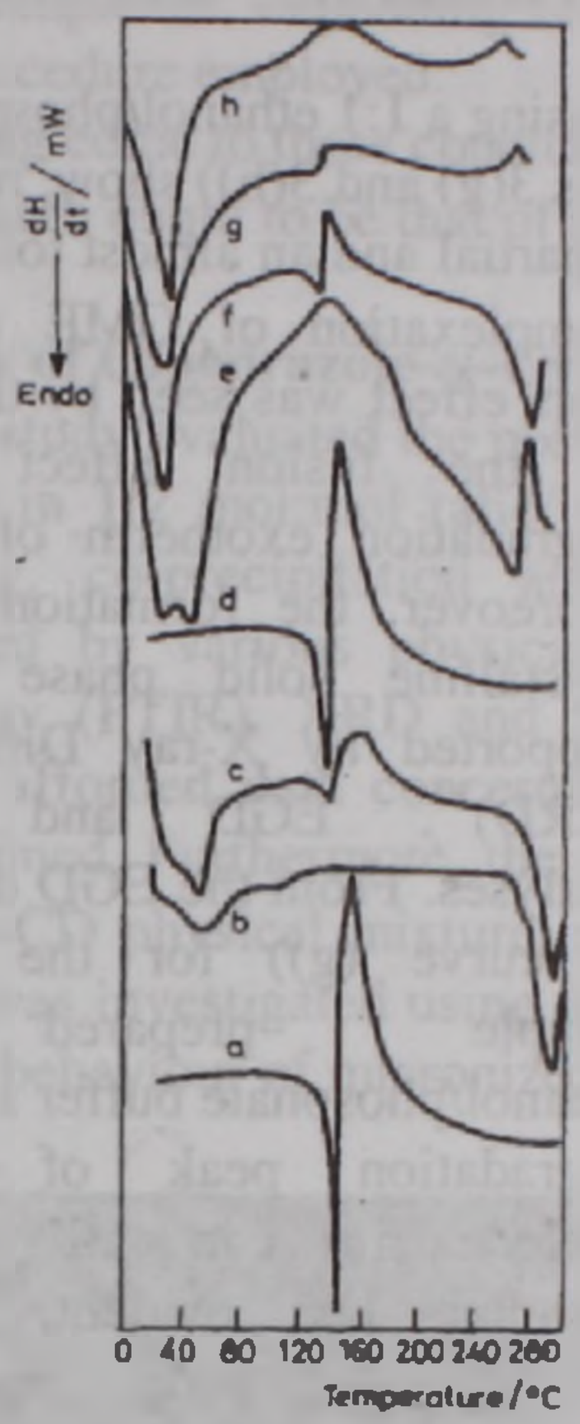

Figure 3. DSC curves corresponding to OME/γ-CD binary systems treated by different co-grinding procedures: (a) micronized OME, (b) γ-CD, (c) physical mixture, (d) dry-ground OME, (e) dry co-ground mixture, and samples obtained by wetting with absolute ethanol (f), 1:1 ethanol/phosphate buffer solution (g) and phosphate buffer (h). (*with kind permission from Kluwer Academic Publishers*)

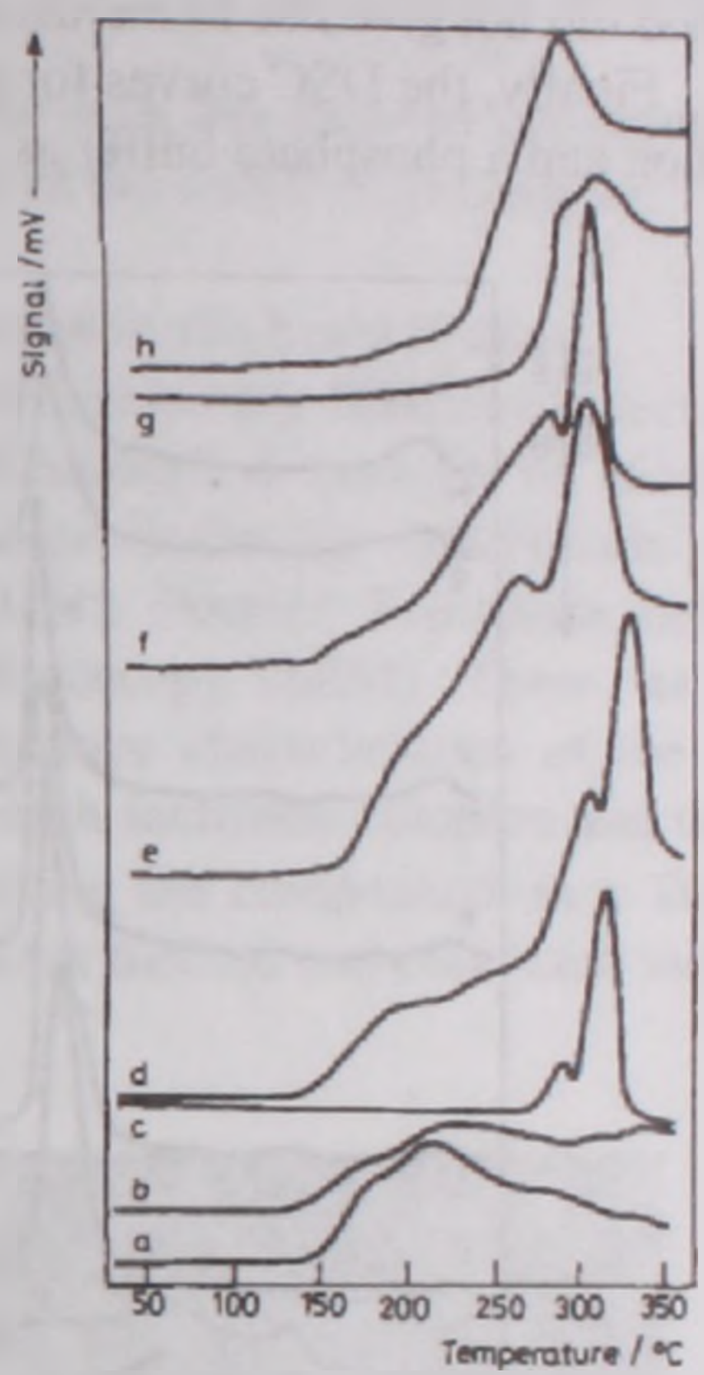

Figure 4. EGD curves corresponding to OME/γ-CD binary systems treated by different co-grinding procedures: (a) micronized OME, (b) γ-CD, (c) physical mixture, (d) dry-ground OME, (e) dry co-ground mixture, and samples obtained by wetting with absolute ethanol (f), 1:1 ethanol/phosphate buffer solution (g) and phosphate buffer (h). (*with kind permission from Kluwer Academic Publishers*)

A drastic change is observed in the thermal profile of the dry co-ground mixture (curve 3(e)). The absence of the characteristic melting peak for OME indicates the presence of an amorphous or poorly crystalline solid state. Although this behaviour has often been interpreted as a consequence of inclusion complex formation, in this case it is probably due to the formation of an amorphous solid dispersion[36]. This assumption, corroborated by the EGD results (Figure 4, curve (e)), agrees with the idea that, the self-absorbed water content of the cyclodextrin host is not normally sufficient to form a real inclusion complex during co-grinding. Moreover, the fact that this inclusion compound was not formed is sustained by the TG/DTG curve (Figure 5, curve (e)), where the mass loss at about 130-140°C has been attributed to degradation of the free drug. As a matter of fact, the TG/DTG profiles, relative to micronized and dry-ground OME and to the OME/γ-CD physical mixture (Figure 5, curves (a), (b) and (d), respectively), display a mass loss over the latter temperature range.

Furthermore the sample obtained by wetting the physical mixture with absolute ethanol (Figure 3, curve (f)), presents the melting endotherm of OME, thus proving that an inclusion compound is not formed when absolute ethanol is used as the binding liquid, suggesting that water is essential for complex formation. In fact, EGD analysis (Figure 4, curve (f)) shows that the sample started to decompose at around 150°C, indicating that this method did not give rise to inclusion complexation.

Finally, the DSC curves for the samples prepared using a 1:1 ethanol/phosphate buffer solution and a phosphate buffer as binding liquids (curves 3(g) and 3(h)) show, respectively, a partial and an almost total inclusion complexation of OME with γ-CD. This effect was seen by the decrease in the fusion effect and the degradation exotherm of the drug. Moreover, the formation of a new crystalline solid phase was also supported by X-ray Diffractometry (XRD)[37], EGD and TG/DTG analyses. From the EGD data (Figure 5, curve (g)) for the co-ground sample prepared with ethanol/phosphate buffer solution, the degradation peak of the free cyclodextrin can still be seen, although less evident, at around 150°C, suggesting only partial complexation. On the other hand, in the case of the sample obtained by using phosphate buffer as the wetting liquid, this thermal event caused by drug decomposition is absent (Figure 5, curve (h)), the only gas evolution effect visible being that at 270°C assigned to complex degradation.

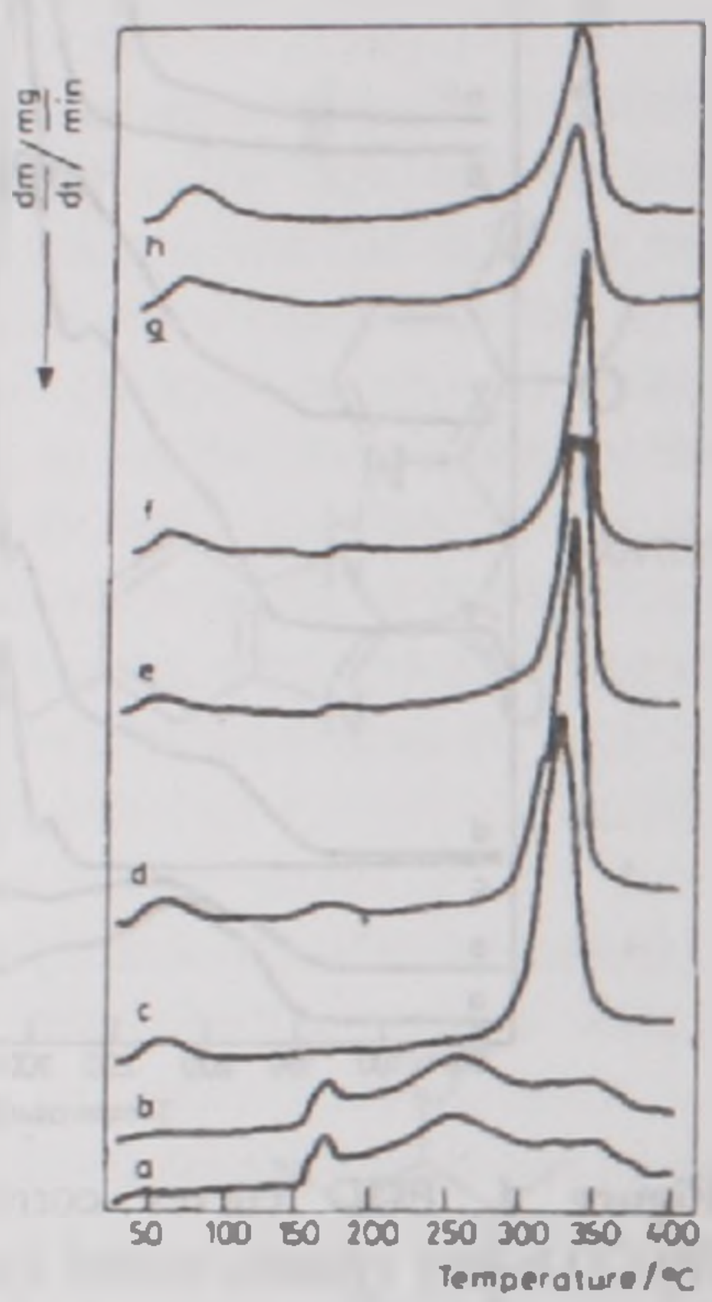

Figure 5. TG/DTG curves corresponding to OME/γ-CD binary systems treated by different co-grinding procedures: (a) micronized OME, (b) γ-CD, (c) physical mixture, (d) dry-ground OME, (e) dry co-ground mixture, and samples obtained by wetting with absolute ethanol (f), 1:1 ethanol/phosphate buffer solution (g) and phosphate buffer (h). (*with kind permission from Kluwer Academic Publishers*)

The feasibility of the formation of an inclusion complex in the co-ground sample prepared with phosphate buffer was corroborated by the HSM data. Crystals of pure OME underwent a melting process at about 159°C, followed by immediate degradation at 162°C. The physical mixture underwent γ-CD dehydration, melting of the drug, partial adsorption of the melt onto the cyclodextrin mass, degradation of the molten drug and finally melting of the γ-CD with decomposition. The same behaviour, although not as pronounced, was observed for the "1:1 ethanol/phosphate buffer solution" sample, whereas melting of the drug was not registered for those samples prepared via dry-grinding and through sole use of phosphate buffer.

In conclusion, all these thermal techniques together revealed that the changed crystalline properties of the composites obtained by co-grinding were due to distinct types of interactions between the components, as a consequence of the variations in the grinding procedure. The experimental data clearly revealed that a true solid complex was obtained

only by wetting the mixtures with a phosphate buffer during co-grinding. Other co-grinding procedures yielded only amorphous drug/cyclodextrin mixtures or their combination with partial complexation. Indeed, since grinding also affects the crystalline properties of a solid, it should be possible to obtain either amorphous mixtures of the co-ground components or inclusion complexes, depending on the characteristics of the starting materials and on the grinding procedure employed.

Having come to these conclusions, it seemed obvious to us that the next step along this line of research ought to be that of studying the solid state of the OME/γ-CD complex.

Study of Omeprazole–γ–Cyclodextrin Complexation in the Solid State

This study evaluated the possibility of obtaining and comparing OME/γ-CD inclusion complexes, in 1:2 mol:mol ratio, using the different technological methods of kneading, spray-drying, co-precipitation and freeze-drying[33]. These inclusion compounds were characterized by various physical methods, such as DSC, Fourier Transform Infrared Spectroscopy (FTIR), XRD and Scanning Electron Microscopy (SEM). These last two techniques afforded data concerning crystallinity and surface characteristics of the solid phases obtained. Furthermore, the dissolution profile of each inclusion complex and that of 1:2 OME/γ-CD physical mixture, prepared by gently mixing the components in a Turbula apparatus, was investigated using the USP 23 rotating basket method and compared with the dissolution behaviour of micronized OME.

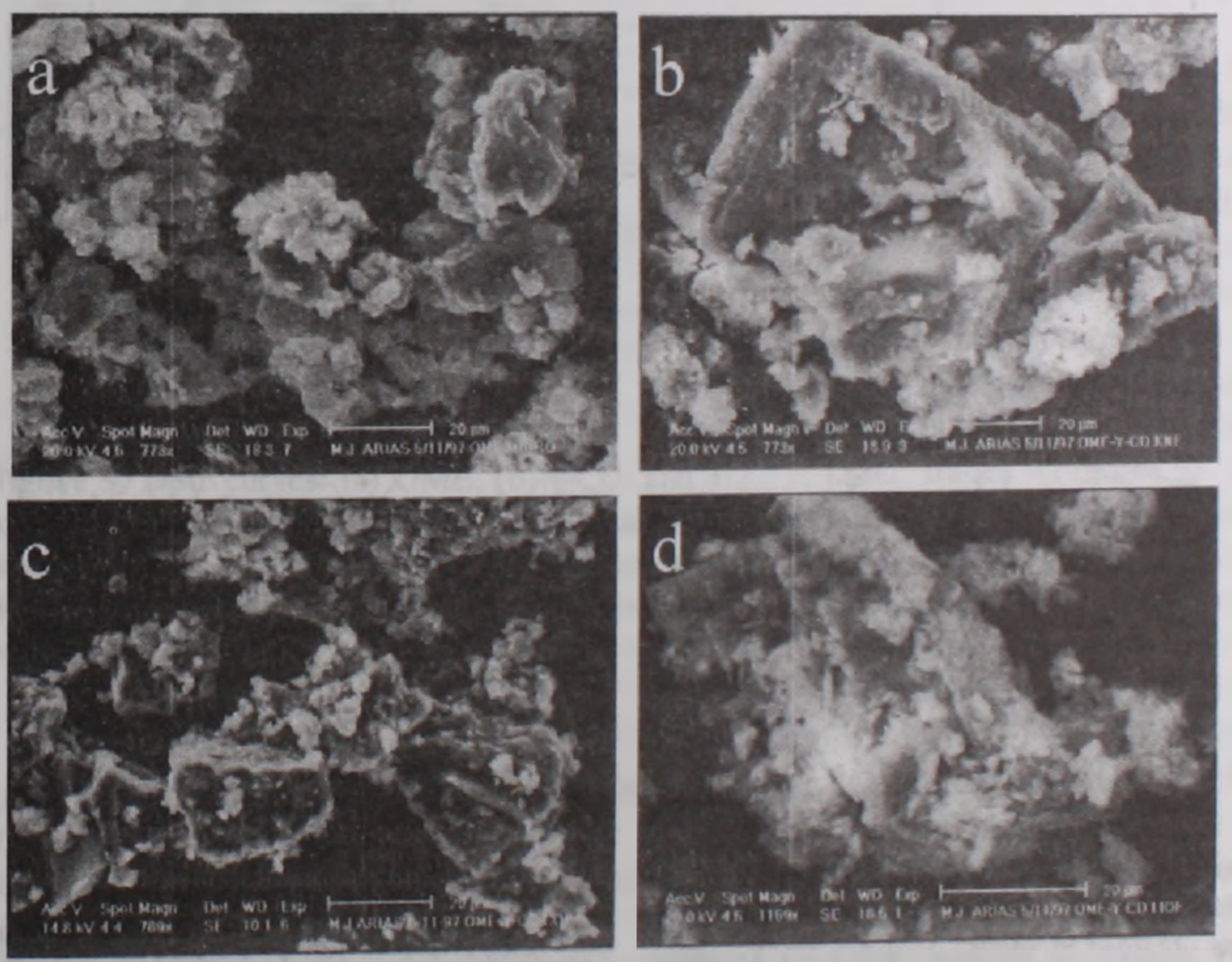

Figure 6. SEM photomicrographs: (a) micronized OME, and 1:2 mol:mol OME/γ-CD systems obtained by kneading (b), co-precipitation (c), and freeze-drying (d). (*with kind permission from Marcel Dekker Inc.*)

Figure 6 shows several SEM photomicrographs of the samples under study. Although this technique is not conclusive for assessing the existence of a true inclusion compound in the solid state, it can be useful to prove the homogeneity of the solid phases. Micronized OME is characterized by the presence of crystalline particles of regular size, while γ-CD appears as crystalline particles without a definite shape (Figure 6, curve (a)). The kneaded system (Figure 6, curve (b)) showed crystalline particles of a single component without any visible drug crystals. A similar morphology was presented by samples prepared via coprecipitation (Figure 6, curve (c)), although in this case the crystals were smaller. The solid phases obtained by freeze-drying (Figure 6, curve (d)) showed a remarkable decrease in crystallinity probably due to the formation of an amorphous inclusion compound. The freeze-dried product appeared to be of a lesser crystalline structure with a soft, fluffy appearance and again, the crystals of the single components were still not distinguishable. The spray-dried sample presented a morphology typical of this preparation i.e. very small, spherical particles with a high tendency to aggregate [24].

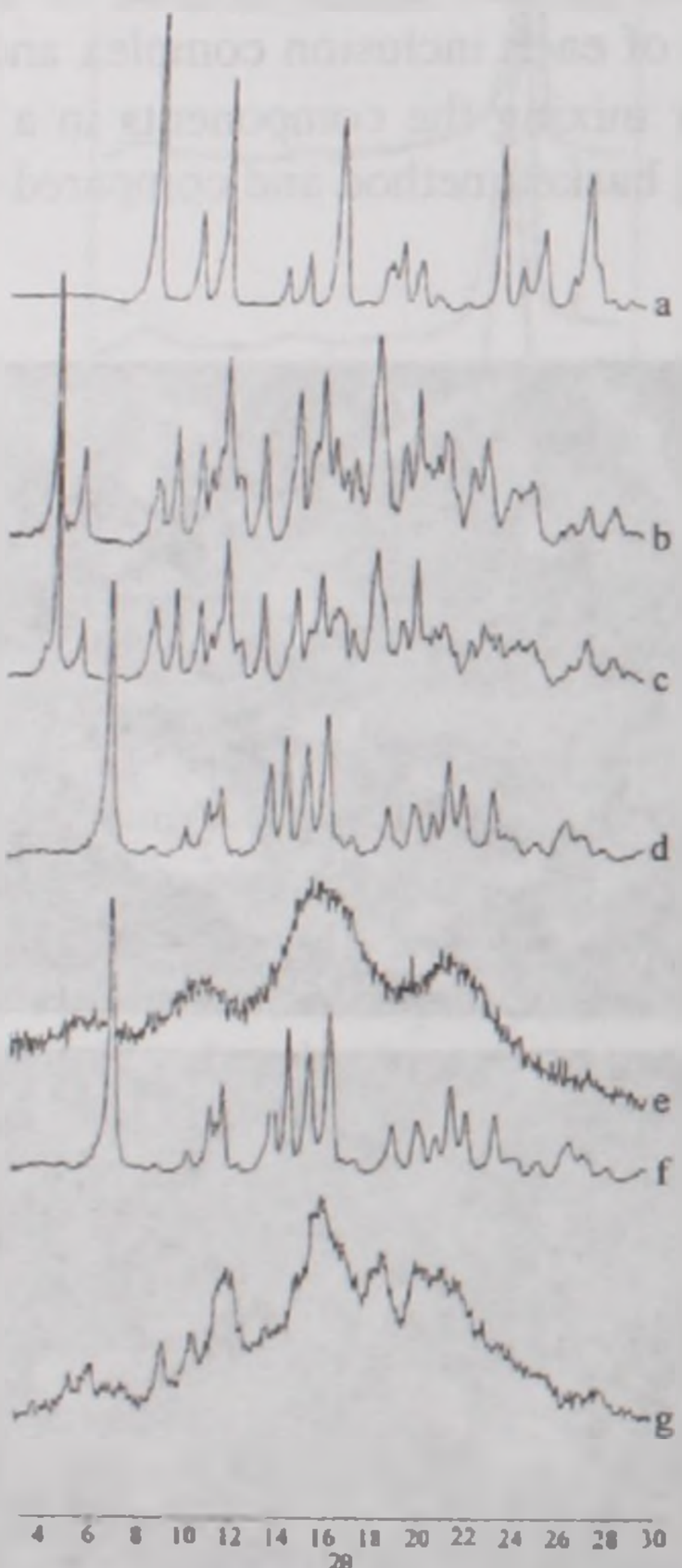

Figure 7. X-ray diffraction patterns on powder: (a) OME, (b) γ-CD, and 1:2 mol:mol OME/γ-CD systems obtained by physical mixing (c), kneading (d), spray-drying (e), co-precipitation (f), and freeze-drying (g). (*with kind permission from Marcel Dekker Inc.*)

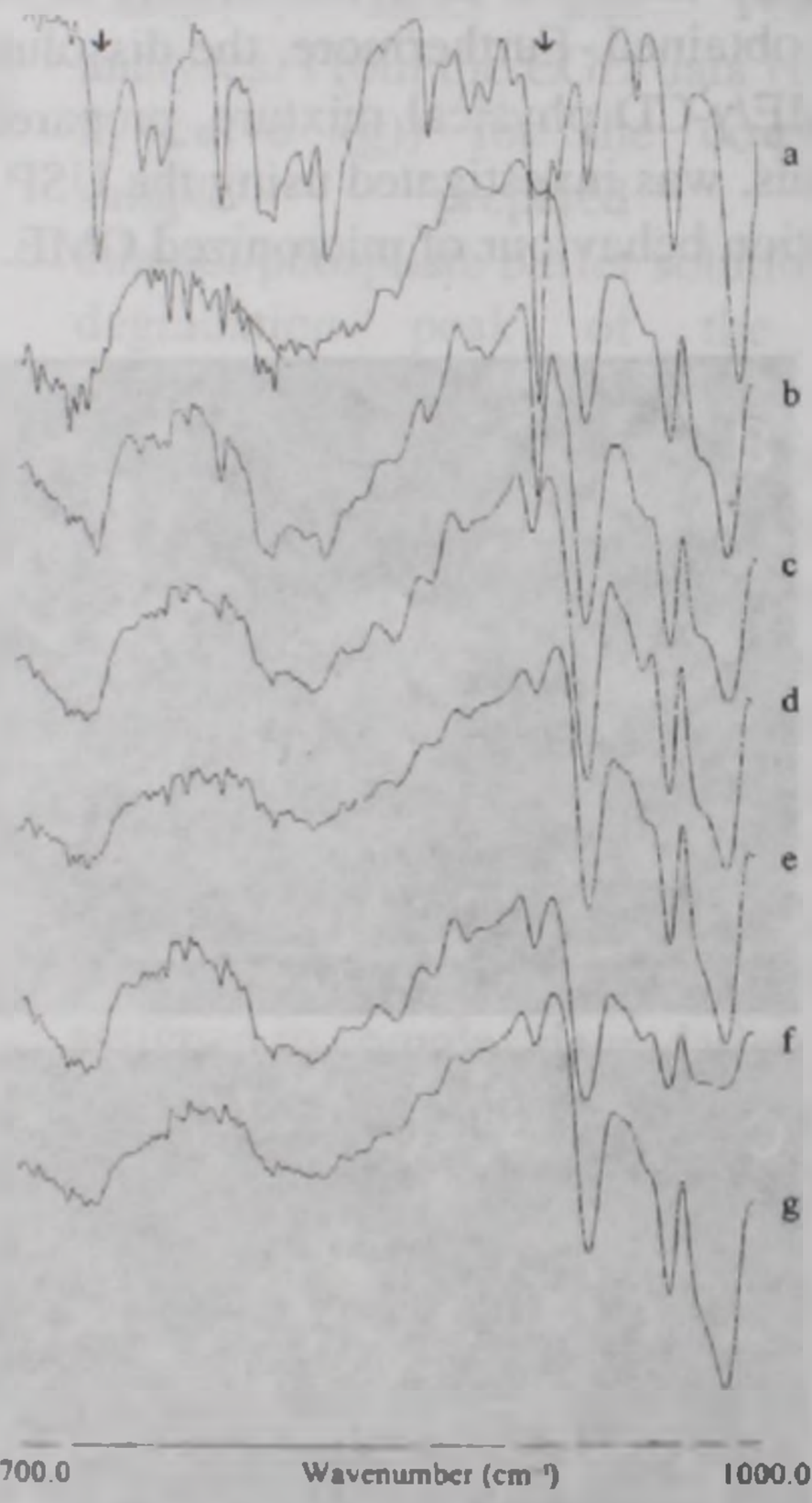

Figure 8. FTIR spectra: (a) OME, (b) γ-CD, and 1:2 mol:mol OME/γ-CD systems obtained by physical mixing (c), kneading (d), spray-drying (e), co-precipitation (f), and freeze-drying (g). (*with kind permission from Marcel Dekker Inc.*)

The X-ray diffraction patterns are depicted in Figure 7. As expected, the physical mixture (curve (c)) corresponds to the simple superposition of the X-ray patterns of OME (curve (a)) and γ-CD (curve (b)). The extremely characteristic diffractograms of the products prepared by kneading and co-precipitation (curves (d) and (f), respectively) probably arose from the formation of a new crystalline phase. The solid phases obtained via freeze-drying (curve (g)) and in particular via spray-drying (curve (e)) showed a remarkable decrease in crystallinity, probably due to the formation of an amorphous inclusion compound. These findings were in-line with those of the FTIR spectral analysis, shown here in Figure 8, where two characteristic bands at 1625.7 cm^{-1} (C=C-N and S-C=N link vibration stretching) [38] and 1204 cm^{-1} (Ar-C-O-CH_3 bending vibration) were chosen from OME's FTIR spectrum to indicate the solid state interactions during complexation. In the spectrum for the physical mixture (curve 8(c)), these two bands remain practically unchanged for position and intensity with respect to the FTIR spectrum of OME alone, indicating that simple mixing did not result in any interaction involving these chromophores. In the FTIR spectra of all the other binary systems, the absorption band at 1625 cm^{-1} disappeared and the intensity of the band at 1204cm^{-1} also markedly decreased probably due to a restriction arising from complexation.

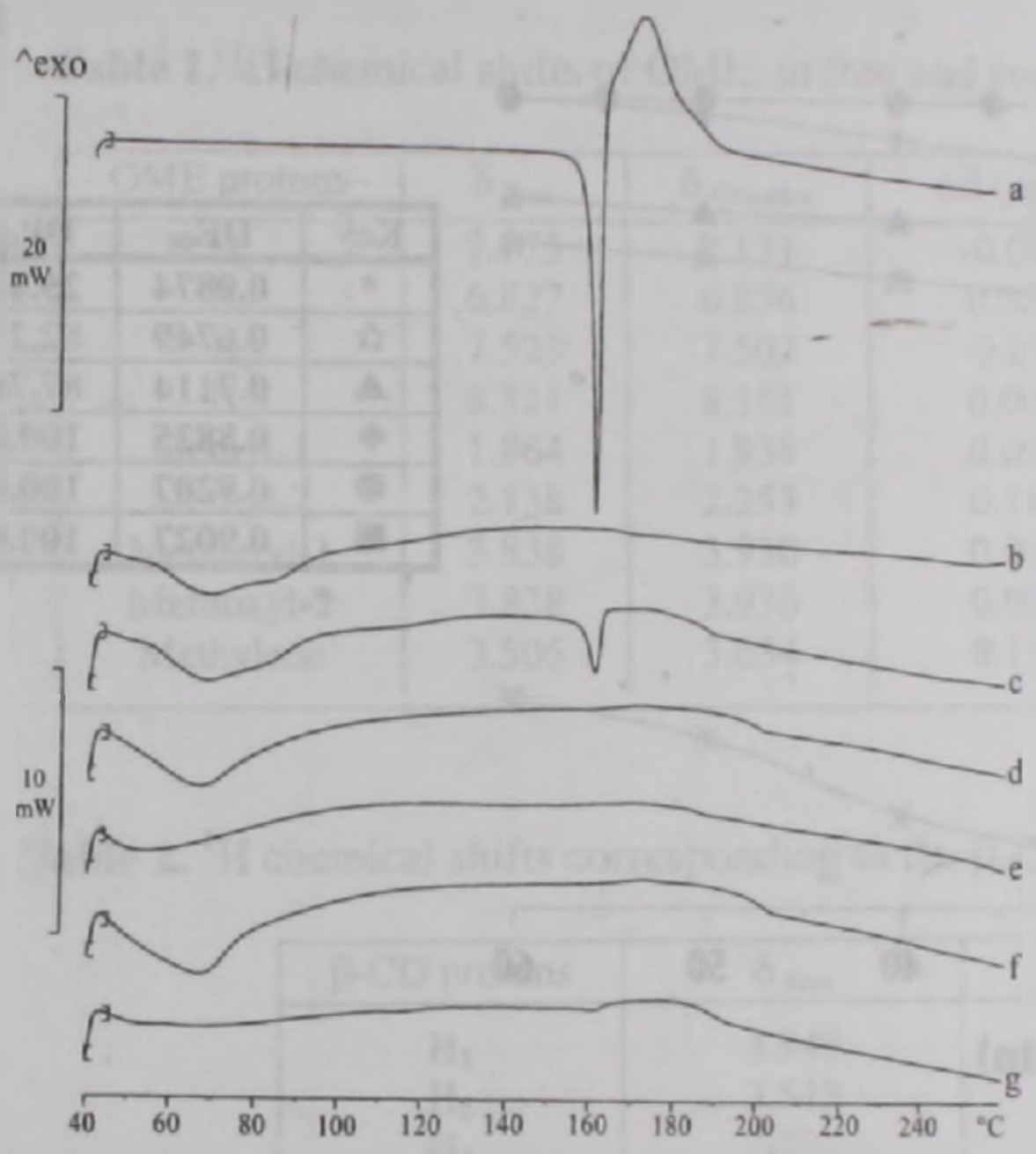

Figure 9. DSC curves: (a) OME, (b) γ-CD, and 1:2 mol:mol OME/γ-CD systems obtained by physical mixing (c), kneading (d), spray-drying (e), co-precipitation (f), and freeze-drying (g). (*with kind permission from Marcel Dekker Inc.*)

The formation of inclusion compounds was confirmed by DSC traces (Figure 9) of the kneaded, spray-dried and co-precipitated systems. Curves (d)-(g) show that the melting endotherm of OME is absent, while it is present in the micronized OME (curve (a)) and in the physical mixture (curve (c)), as expected. However, a residual endothermic effect at around 161°C is observed in the run of the freeze-dried sample, indicating that a small fraction of crystalline free OME is still present, corresponding to approximately 3.5% of the sample.

The dissolution profiles for the systems under study are depicted in Figure 10. For their evaluation two parameters, dissolution efficiency[39] and the percentage of drug dissolved after 60 min (DE_{60} and DP_{60}, respectively), were measured. Among the solid phases obtained, the co-precipitated and the freeze-dried products presented the highest dissolution rates with complete dissolution being achieved within approximately 20 minutes, while the product of spray-drying had a lower dissolution rate. This may be attributed to the high tendency of the

spherical particles to agglomerate in the spray-dried form, probably due to the presence of electrostatic forces. The low DE_{60} and DP_{60} values for the kneaded product could, on the other hand, be traced to the self-aggregation of particles which reduces the surface area available for dissolution. Finally, the physical mixture also shows a significant enhancement in OME dissolution rate with respect to OME alone. This may be ascribed to two concomitant effects, the improved wettability of the physical mixture brought about by the presence of γ-CD, a highly hydrophilic component, and to the possible formation *in situ* of the relevant inclusion compound when the physical mixture comes into contact with the dissolution medium.

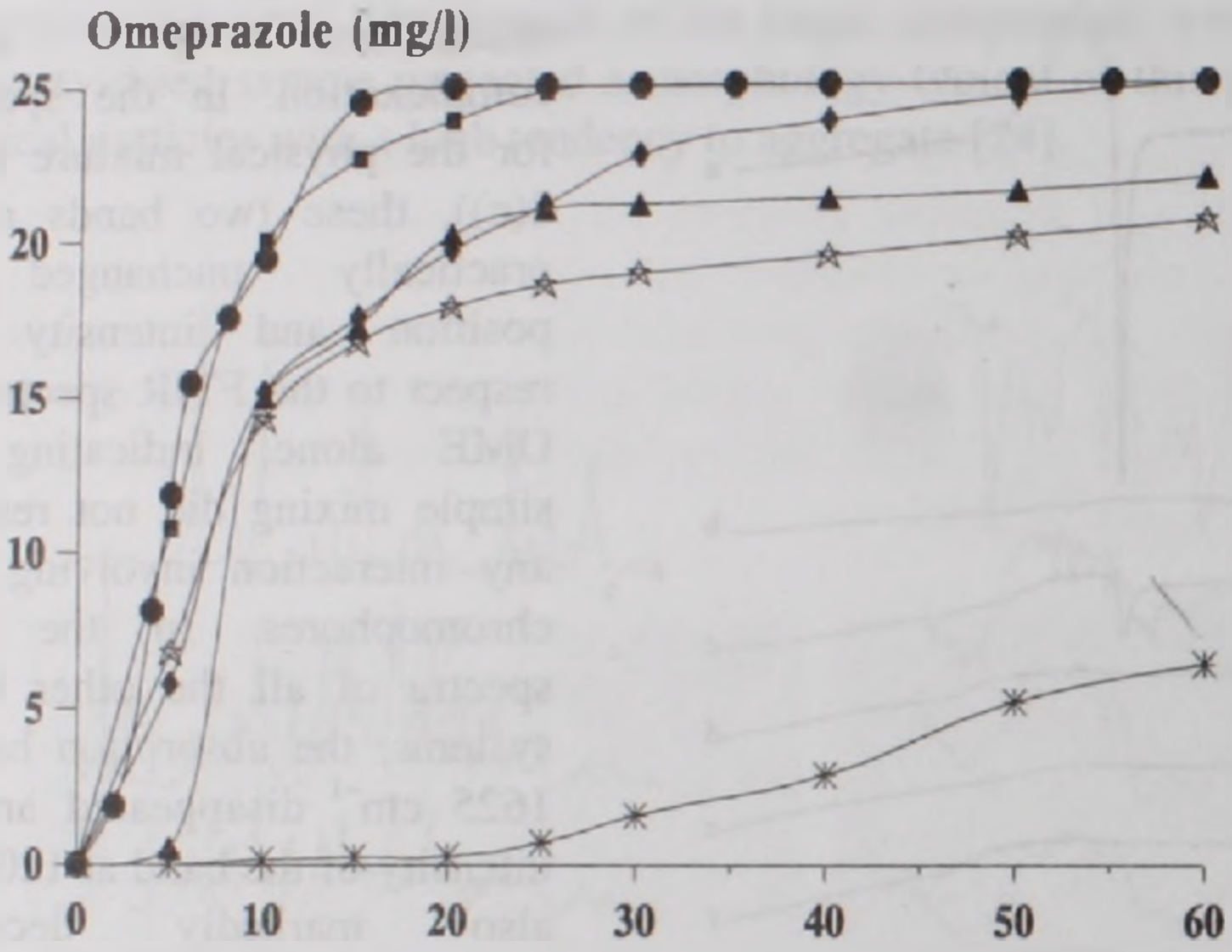

Key	DE_{60}	DP_{60}
*	0.0874	25.44
☆	0.6749	82.25
▲	0.7114	87.74
◆	0.8825	100.0
●	0.9207	100.0
■	0.9027	100.0

Figure 10. Dissolution curves and dissolution parameters of micronized OME and 1:2 mol:mol OME/γ-CD systems (* OME, ☆ physical mixture, ▲ kneaded, ◆ spray-dried, ● co-precipitated and ■ freeze-dried). (*with kind permission from Marcel Dekker Inc.*)

Having successfully prepared and thoroughly characterized OME/γ-CD inclusion compounds, we were eager and ready to proceed with our research and to study the complexation properties of β-CD with OME in aqueous media.

Investigation of the Inclusion Complex Formation between Omeprazole and β–Cyclodextrin by Phase-solubility Analysis, ^{1}H and ^{13}C NMR Spectroscopies and Molecular Modelling.

This third section reports the investigation of the complexation mechanism and the driving forces involved in the interaction between OME and β-CD in aqueous media[26,34,40]. The effect of host concentration on apparent guest solubility, the possible separation of solid complexes, their stoichiometric ratios in solution and in the solid state, the calculation of apparent stability constants and the molecular geometry of the relative inclusion compounds were all aspects of complexation that were thoroughly examined in this study using techniques of Phase Solubility Analysis, ^{1}H and ^{13}C NMR Spectroscopy and Molecular Modelling.

In the outcome of the guest molecule being included within the host molecule, the NMR spectra of the inclusion compound will differ, in terms of chemical shift values, from both that of the sole guest molecule and that of the cyclodextrin itself.

The ^{1}H NMR spectral data of the drug and β-CD both in the free and complexed states are reported in Tables 1 and 2, respectively. The peak assignments for OME are shown in Figure 11 and those for β-CD are shown in Figure 12. In the case of the cyclodextrin host, the greatest differences in chemical shift ought to be encountered for those protons situated within the hydrophobic cavity as they will experience this shielding effect the most once the guest molecule has been included whereas, any possible external guest/host interaction will not alter these chemical shifts. This was found to be true for host protons H5 and H6, situated towards the narrower rim of the internal surface.

Table 1. ^{1}H chemical shifts of OME, in free and complexed states in $NaOD/D_2O$ solution.

OME protons	δ_{Free}	$\delta_{Complex}$	$\Delta\delta$ (ppm)	Peak multiplicity
H_a	7.173	7.171	-0.002	doublet (coupled with H_b)
H_b	6.827	6.856	0.029	doublet (coupled with H_a)
H_c	7.523	7.502	-0.021	doublet
H_d	8.121	8.181	0.060	singlet
Methyl-1	1.864	1.958	0.094	singlet
Methyl-2	2.138	2.253	0.115	singlet
Methoxyl-1	3.838	3.930	0.092	singlet
Methoxyl-2	3.838	3.930	0.092	singlet
Methylene	3.505	3.634	0.129	singlet

Table 2. ^{1}H chemical shifts corresponding to the β-CD, in the presence and absence of OME.

β-CD protons	δ_{Free}	$\delta_{Complex}$	$\Delta\delta$ (ppm)
H_1	4.949	4.969	0.020
H_2	3.513	3.531	0.018
H_3	3.875	3.878	0.003
H_4	3.427	3.448	0.021
H_5	3.802	3.765	-0.037
H_6	3.870	3.803	-0.067

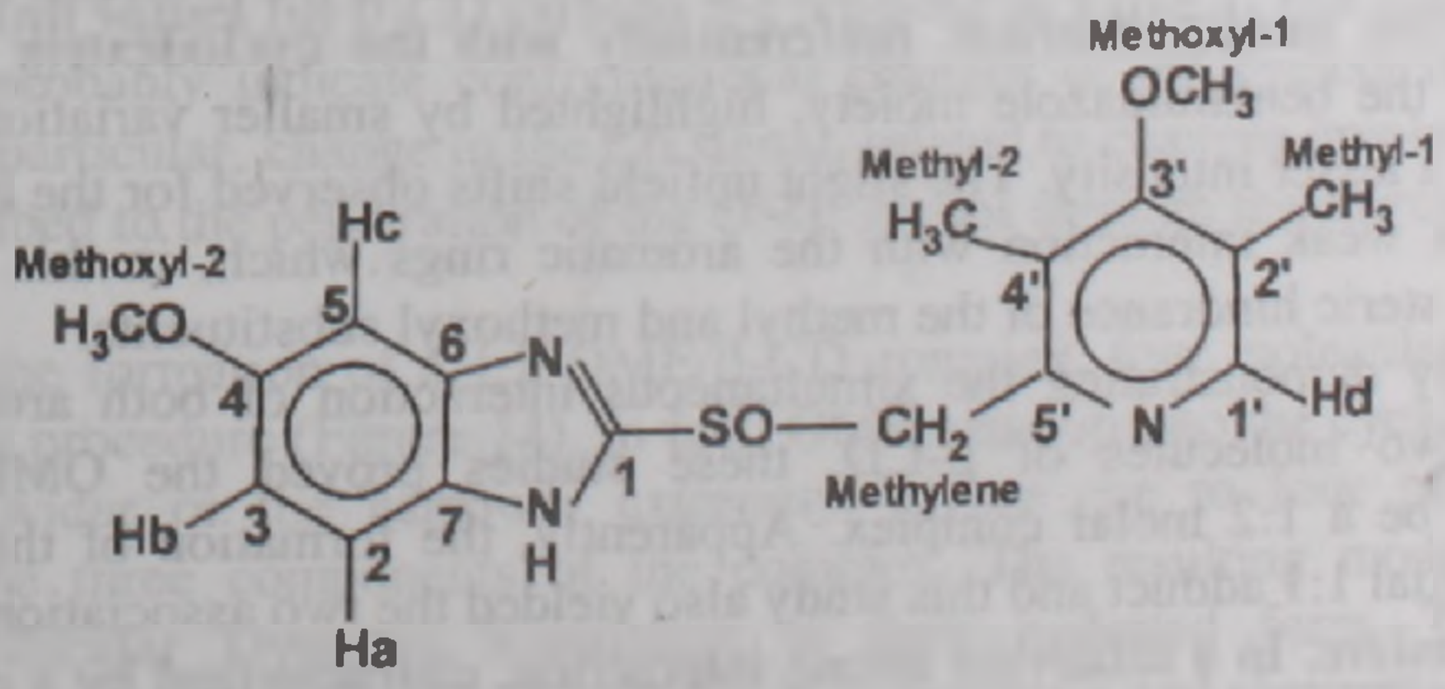

Figure 11. Structure and labelling scheme of OME.

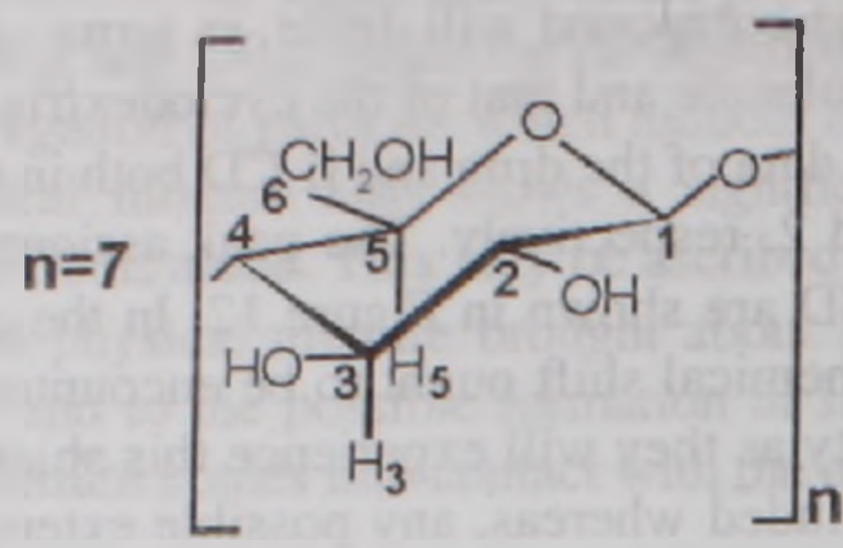

Figure 12. Labelling scheme of β-CD.

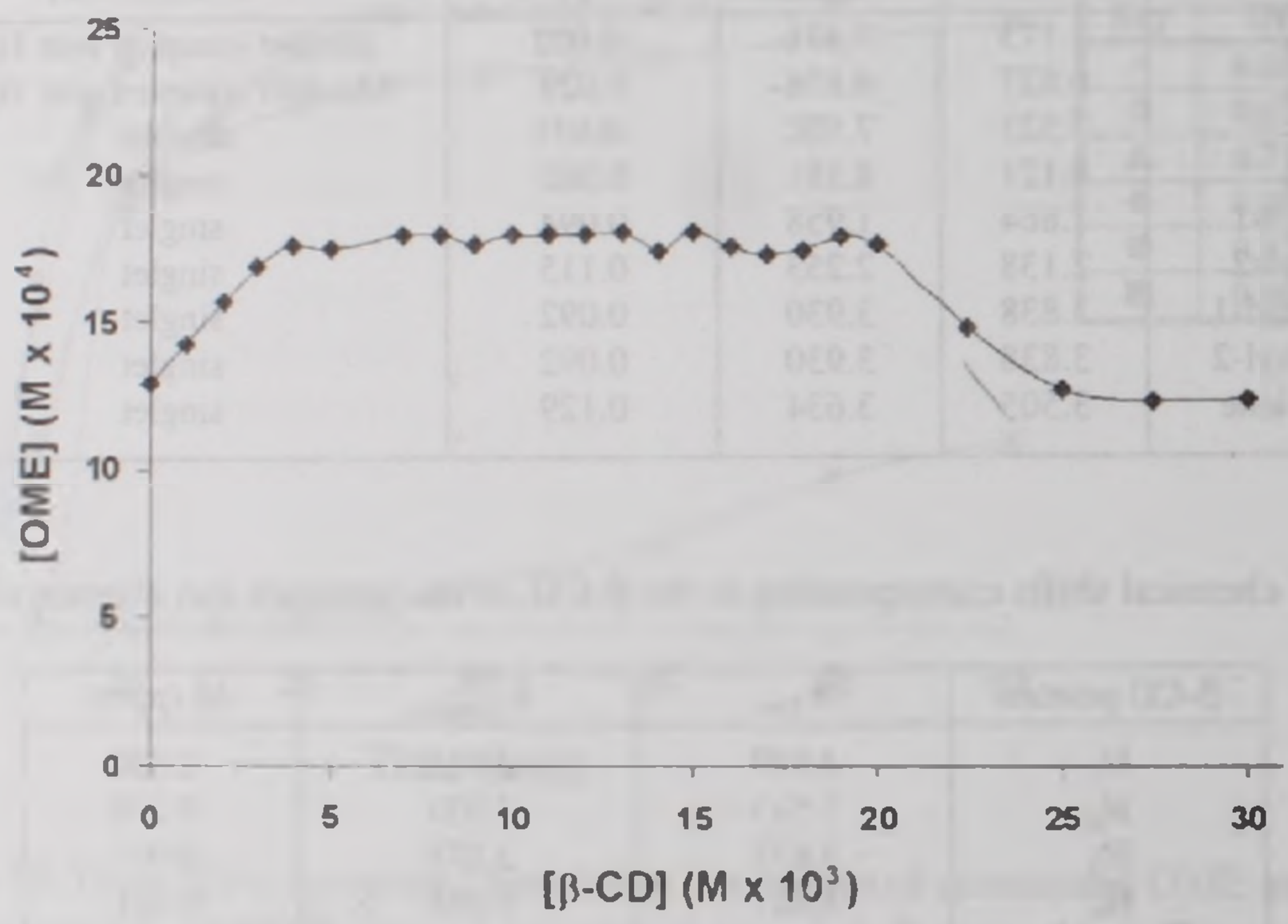

Figure 13. Phase-solubility diagram of OME in presence of β-CD at 25 °C.

The observed downfield shifts of the guest protons in the presence of β-CD, indicated that the pyridine moiety interacts preferentially with the cyclodextrin cavity, while the interaction of the benzimidazole moiety, highlighted by smaller variations in its chemical shifts, was of a lesser intensity. The slight upfield shifts observed for the inner protons of β-CD indicate a weak interaction with the aromatic rings which, in this case, is probably caused by the steric hindrance of the methyl and methoxyl substituents.

Thus, by demonstrating the simultaneous interaction of both aromatic portions of OME with two molecules of β-CD, these studies proved the OME/β-CD inclusion compound to be a 1:2 molar complex. Apparently, the formation of this complex passes through an initial 1:1 adduct and this study also yielded the two association constants for this stepwise procedure. In a relatively strong interaction, characterized by a constant $K_1 = 92.6$ M^{-1}, the pyridine moiety of the guest molecule becomes entrapped by a first host molecule, and the benzimidazole moiety of the guest then accommodates itself within a second host molecule to give the 1:2 complex. However, a second relatively low association constant (K_2

= 4.4 M^{-2}) suggests a rather weak interaction. Initial formation of a 1:1 complex is further supported by the phase-solubility curve (Figure 13). The ascending linear portion has a slope < 1, indicating that the increase in the apparent solubility of OME is most probably due to the formation of an equimolar complex.

The hypothesis that the pyridine portion has a higher affinity for the cyclodextrin cavity than the benzimidazole moiety does, is sustained by ^{13}C NMR data. The ^{13}C NMR chemical shifts for omeprazole carbons, both free and complexed, are shown in Table 3. As a rule, the guest carbons lining the cavity are shielded, while those situated near the rim are deshielded. The observed upfield chemical shifts of several pyridine carbon atoms indicate its inclusion by the cyclodextrin. On the other hand, the downfield shifts observed for C3' and C5' atoms suggest that these carbons are positioned towards the outside of the cavity, and indicate the degree of penetration into the host. Furthermore, upfield shifts were observed for C3 and C5 of the benzimidazole moiety, whereas the signal of C1 was shifted downfield, indicating only partial penetration.

Table 3. ^{13}C chemical shifts of OME in free and complexed states in $NaOD/D_2O$ solution.

OME carbons	δ_{Free}	$\delta_{Complex}$	$\Delta\delta$ (ppm)
C_1	155.344	155 621	0.277
C_2	100.318	100.530	0.212
C_3	112.340	111.954	-0.386
C_4	148.783	n.a.	n.a
C_5	118.743	118.510	-0.233
C_6	141.118	141.135	0.017
C_7	146.453	146.242	-0.211
C_1'	149 538	149 490	-0 048
C_2'	127.650	126.891	-0.759
C_3'	164.772	165.011	0 239
C_4'	128.582	128.189	-0.393
C_5'	158.733	159.171	0.438
Methyl-1	11.292	11.551	0 259
Methyl-2	13.134	13.787	0.653
Methoxyl-1	60.694	n.a.	n.a
Methoxyl-2	60.694	n.a.	n.a
Methylene	56.614	57.472	0.858

Chemical shift values for β-CD carbons are reported in Table 4. The observed shifts of C1, C4 and C6 probably indicate conformational changes of the cyclodextrin ring upon complexation. In particular, change in the C6 signal, related to changes involving the C5-C6 bond, can be ascribed to the penetration of the OME groups through the narrow extremity of the β-CD.

Assuming the formation of a 1:2 OME/β-CD complex, four molecular models were built by a docking procedure (Figure 14). In fact, OME can slip into the cyclodextrin cavity either from the wider or the narrower extremity, giving rise to four putative mutual orientations of the three components of the complex. The resulting models were then submitted to Molecular Dynamic Simulation in their hydrated form. The following parameters were calculated and reported in Table 5: i) the steric and electrostatic interaction energy between OME and the two host molecules; ii) the distances between OME's centre of mass and those of the two β-CD molecules. Figure 15 depicts the average coordinates of the

four models. From these data, host molecule CD1 seems to bind more firmly to the pyridine ring than CD2 does to the benzimidazole group. This is explained by molecular dynamic studies as being due to the wider dimensions of the substituted pyridine group, which stops the β-CD molecule from "slipping off". In models (b) and (c), strong electrostatic interactions occur between the polar core of OME and the secondary hydroxyl groups of β-CD which could explain why the association constant for the 1:1 complex is greater than that of the 1:2 complex. These observations are consistent with ^{1}H NMR and ^{13}C NMR data. As for the mutual arrangement of the complex constituents, the computational results do not provide indications about a strong preference between the two possible orientations of CD1. Nevertheless, when oriented as in models (b) and (c), CD1 shifted towards OME's centre, thus generating repulsive forces with the second β-CD molecule. On its own, CD2 interacts with OME to a lesser extent when inserted from the wider side as depicted in models (b) and (d). In model (b), where these two conditions are combined, CD2 is completely lost at the end of the simulation.

Table 4. ^{13}C chemical shifts corresponding to the β-CD, in the presence and absence of OME.

β-CD carbons	δ_{Free} (ppm)	$\delta_{Complex}$ (ppm)	$\Delta\delta$ (ppm)
C_1	103.576	103.501	-0.075
C_2	73.828	73.760	-0.068
C_3	74.662	74.722	0.060
C_4	82.556	82.293	-0.263
C_5	72.630	72.676	0.046
C_6	61.238	60.901	-0.337

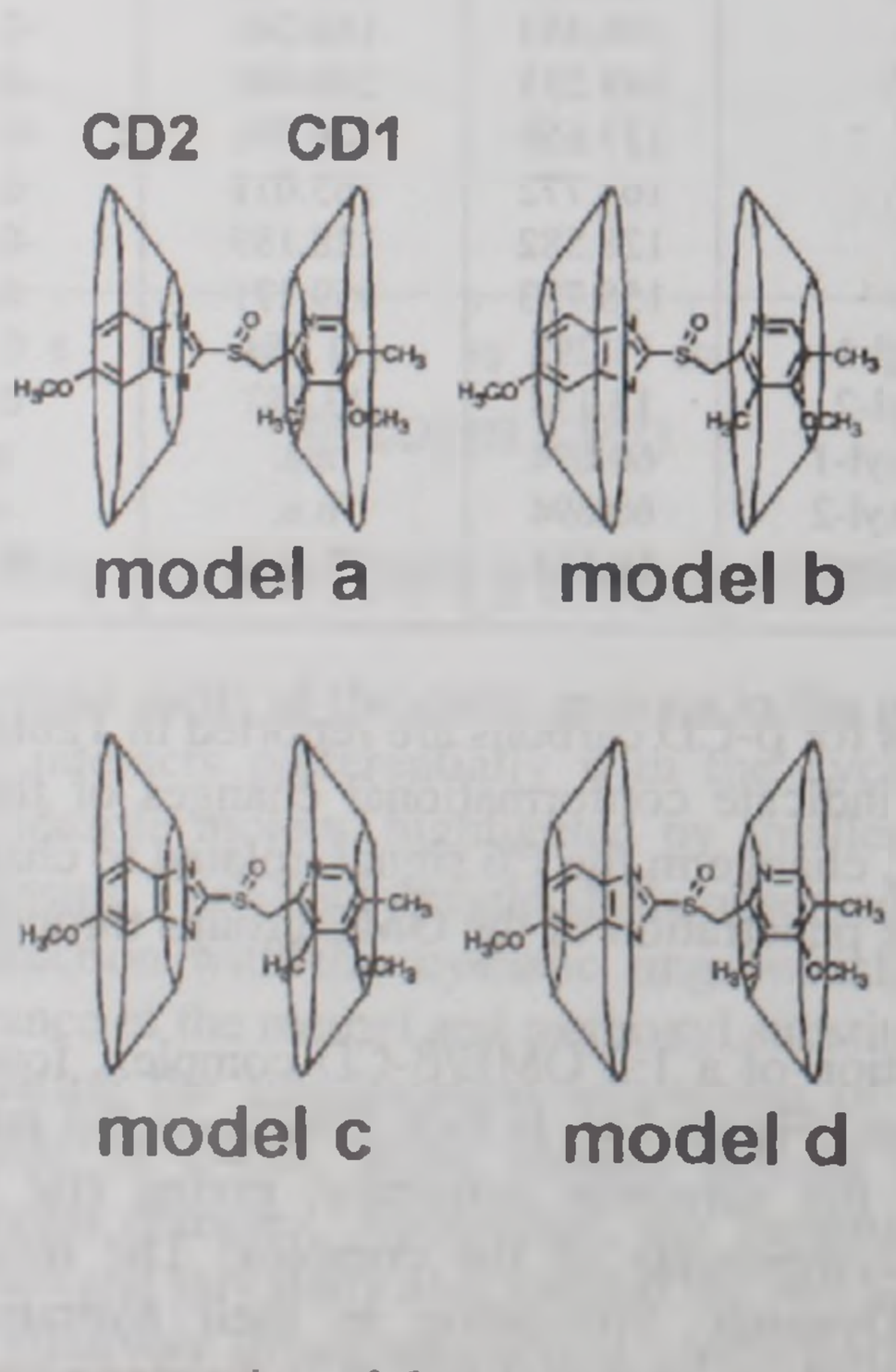

Figure 14. Schematic representation of four molecular models of the OME/β-CD inclusion compound.

Table 5. Molecular dynamics results. Mean values (s.d.) of the distances between OME and β-CD centers of mass, and of calculated interaction energies (CD1 from the pyridine side, CD2 from the benzimidazole side), measured over the last 30 picoseconds of the analysis

Model	Dist. (Å)	CD1 Electrostatic (kcal/mol)	Steric (kcal/mol)	Dist (Å)	CD2 Electrostatic (kcal/mol)	Steric (kcal/mol)
A	3.89 (0.25)	−7.41 (1.47)	−19.43 (2.56)	7.01 (0.38)	−1.43 (2.88)	−16.15 (1.34)
B	1.22 (0.33)	−18.22 (3.94)	−23.82 (1.53)	19.93 (0.57)	0.17 (0.37)	−0.07 (0.05)
C	1.33 (0.30)	−20.45 (2.41)	−21.69 (1.69)	10.21 (0.37)	−6.27 (2.96)	−7.49 (1.47)
D	3.08 (0.22)	−12.02 (1.95)	−23.22 (2.03)	11.43 (0.47)	−0.61 (1.14)	−2.88 (1.17)

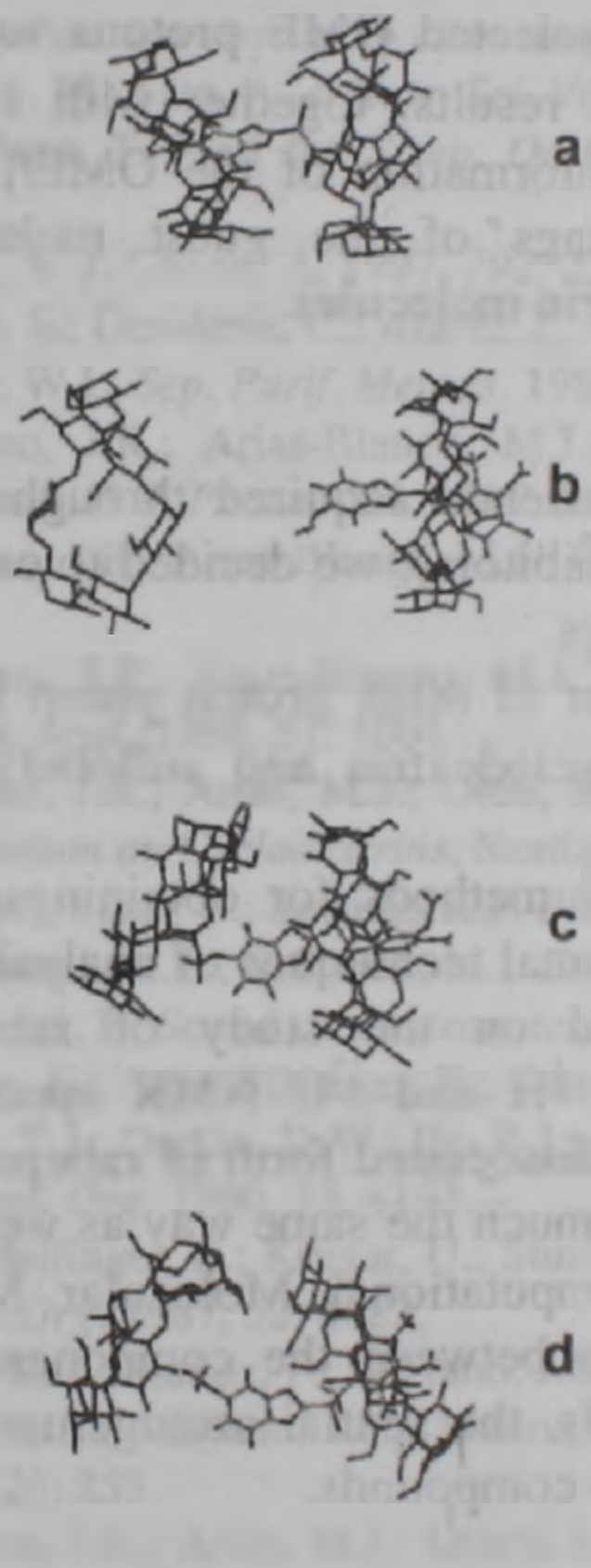

Figure 15. Molecular dynamics average structures of models (a)-(d).

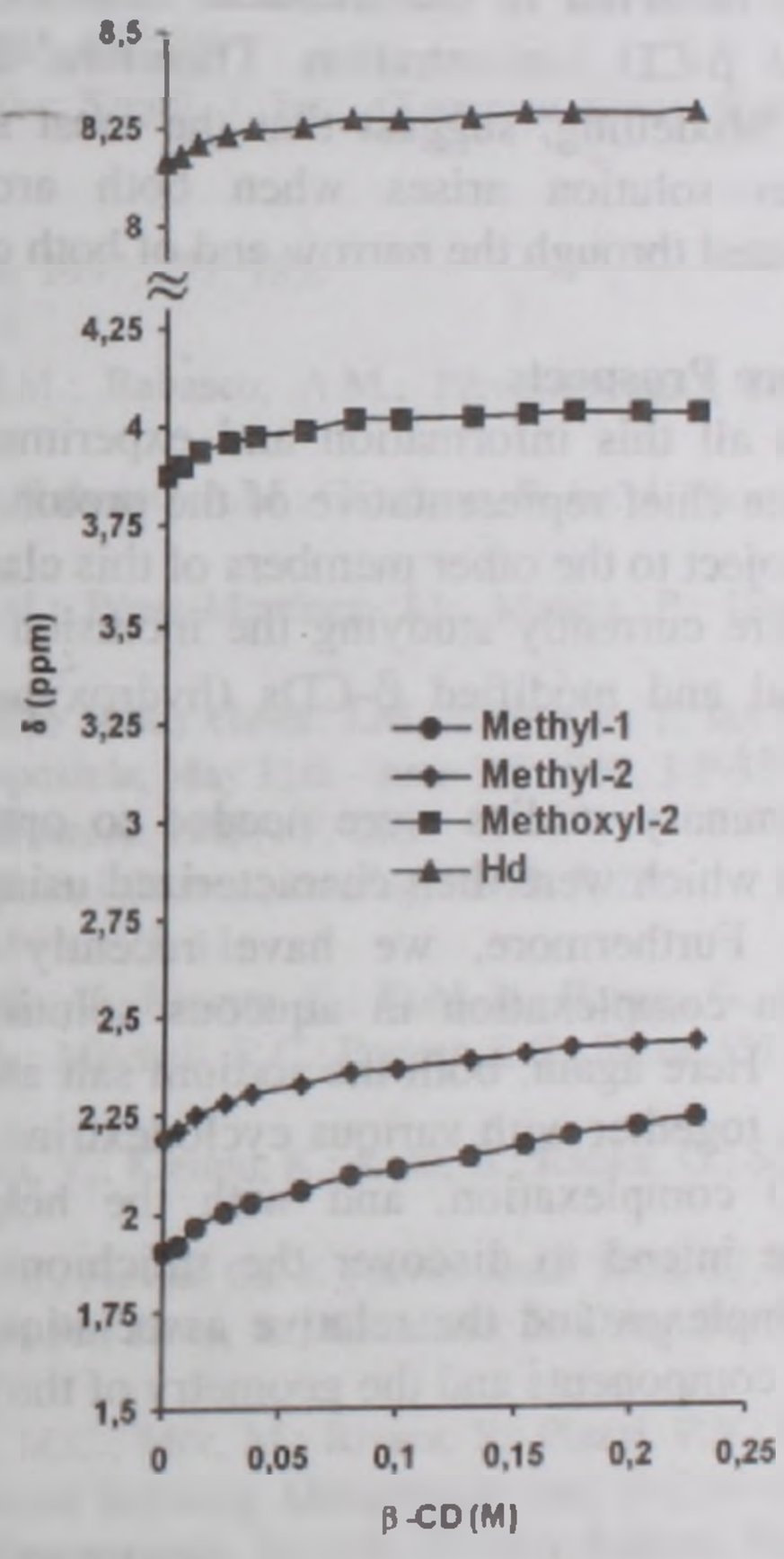

Figure 16. Plot of chemical shift changes of selected protons of OME *vs* the CD concentration.

Therefore, more than one mutual arrangement could be present in solution, and the NMR behaviour could be the result of different situations. Moreover, if CD1 is oriented as in models (a) and (d), the complexation of CD2 around the benzimidazole seems to be favoured, particularly if this is inserted from the narrower rim. Model (a) could therefore explain the chemical shift displacements for OME: the largest ^{1}H and ^{13}C chemical shift variations, observed for the methylene and methyl signals, could be due to the fact that these nuclei are surrounded by the narrower and the wider rim of CD1, respectively (Figure 15). This could also explain the downfield shifts of the corresponding ^{13}C signals, due to interactions with the β-CD rims, and the upfield shifts of the pyridine C1', C2' and C4' signals, considering that these atoms lie within the β-CD cavity. On the contrary, when CD1 is oriented as in models (b) and (c), the methylene group is positioned inside the β-CD hydrophobic cavity and its ^{13}C signal should experience an upfield shift. For the β-CD chemical shift displacements, the highest values were observed for H5, H6 and C6, indicating stronger interactions with the narrower rim, as in model (a). Figure 16 shows how the change observed in the chemical shift values for selected OME protons varies as a function of β-CD concentration. Therefore, the NMR results, together with studies of Molecular Modelling, suggest that the most stable conformation of the OME/β-CD 1:2 complex in solution arises when both aromatic rings of the guest molecule are accommodated through the narrow end of both cyclodextrin molecules.

Future Prospects.

With all this information and experimental experience acquired through studying OME (as the chief representative of the proton pump inhibitors), we decided to extend this research project to the other members of this class of drugs.

We are currently studying the inclusion behaviour of other proton pump inhibitors with natural and modified β-CDs (hydroxypropyl-β-cyclodextrin and sulfobutylether-β-cyclodextrin).

Preliminary studies were needed to optimize the methods for obtaining inclusion compounds which were then characterized using the thermal techniques of analysis already mentioned. Furthermore, we have recently embarked on the study of rabeprazole-cyclodextrin complexation in aqueous solution, using ^{1}H and ^{13}C NMR spectroscopic techniques. Here again, both the sodium salt and the undissociated form of rabeprazole are considered, together with various cyclodextrins. In very much the same way as we did with OME/β-CD complexation, and with the help of Computational Molecular Modelling Studies, we intend to discover the stoichiometric ratio between the components of the various complexes and the relative association constants, the spatial arrangements of the interacting components and the geometry of the inclusion compounds.

REFERENCES

1. Villiers A. *C.R. Hebd. Sciences Acad. Sci.*, Paris, 1891, *112*, 536.
2. Schardinger, F. Z. *Unters. Nahr.u.Genussm.*, 1903, 6, 865.
3. Szejtli, J. *Cyclodextrin Technology*; Kluwer Academic Publishers, Dordrecht, 1998.
4. Duchêne, D. *New Trends in Cyclodextrins and their Derivatives*; Ed.; Editions de Santé, Paris, 1991.
5. Bender, M.I.; Komiyama, M. *Cyclodextrin Chemistry*; Springer Verlag, 1978, Berlin-Heidelberg-New York.
6. Stella, V.J; Rajewski, R.A. *Pharm. Res.* 1997, *14*, 556.
7. Menard, F.A.; Dedhiya, M.G.; Rhodes, C.T. *Drug Dev. Ind. Pharm.* 1990, *16*, 91.

8. Bergeron, R.J. in *Inclusion Compounds*; Atwood, J.L.; Davies, J.E.D.; MacNicol, D.D. Eds.; Academic Press, London, 1984; Chapter 12, 391.
9. Saenger, W. in *Inclusion Compounds*; Atwood, J.L.; Davies, J.E.D.; MacNicol, D.D. Eds.; Academic Press, London, 1984; Chapter 8.
10. Thompson, D.O. in *Cyclodextrins-enabling excipients: Their present and future use in Pharmaceuticals*. Buck, S. Ed., Critical Reviews in Drug Carrier Systems, CRC Press 1997.
11. Rajewski, R.A.; Stella, V.J. *J. Pharm. Sci.* 1996, *85*, 1142.
12. Loftsson, T.; Brewster, M.E. *J. Pharm. Sci.* 1996, *85*, 1017.
13. Frömming, K.H.; Szejtli, J. *Cyclodextrins in Pharmacy*; Kluwer Academic Publishers, Dordrecht, 1994.
14. Szejtli, J., Past, Present and Future of Cyclodextrin, What's New in Cyclodextrin Drug Delivery? Palais des Congrès, Porte Maillot, France, July 7-8, 2000.
15. Szente, L. in *Stability Testing in the EEC, Japan and the USA. Scientific and Regulatory Requirements*. Grimm, W.; Krummen, K. Eds.; Wissenschaftliche Verlagsgesellschaft: Stuttgart, 1993, 225.
16. Duchêne, D. *Cyclodextrins and their Industrial uses*. Ed.; Editions de Santé, Paris, 1987.
17. Sunstar Inc. *Non irritating cosmetics*. Japanese Patent – –10323, 1984.
18. Suzuky, M.; Sato, A. *J. Nutr. Sci. Vitaminol.* 1985, *31*, 209.
19. Fukinbara, T. *First Int. Symp. On Cyclodextrins*; Szejtli, J. Ed.; Akademiai Kiado, Budapest, 1982, 480.
20. Fanali, S. *J. Chrom. A.* 1997, *792*, 227.
21. Fanali, S.; Desiderio, C.; Aturki, Z. *J. Chrom. A.* 1997, *772*, 185.
22. Hinze, W.L. *Sep. Purif. Metods*. 1981, *10*, 1093.
23. Moyano, J.R.; Arias-Blanco, M.J.; Ginés, J.M.; Rabasco, A.M.; Pérez-Martínez, J.I.; Mor, M.; Giordano, F. *J. Pharm.* Sci. 1997, *86*, 72.
24. Moyano, J.R.; Arias-Blanco, M.J.; Ginés, J.M.; Rabasco, A.M.; Giordano, F. *Int. J. Pharm.* 1997, *148*, 211.
25. Moyano, J.R.; Arias-Blanco, M.J.; Ginés, J.M.; Pérez-Martínez, J.I.; Muñoz, P.; Giordano, F. *J. Therm. Anal.* 1998, *51*, 1001.
26. Moyano, J.R.; Arias, M.J.; Ortiz, M.C.; Garrido, M.A.; Ginés, J.M.; Giordano, F. *9th International Symposium on Cyclodextrins*, Santiago de Compostela, May 31th - June 3rd 1998, 3-P-31.
27. Beil, W.; Staar, U.; Sewing, K.F. *Biochem. Pharmacol.* 1988, *37*, 843.
28. Shamburek, R.D.; Schubert, M.I. *Bailliere's Clinical Gastroenterology* 1993, *7*, 23.
29. Wallmark, B. *Scand. J. Gastroenterol. Suppl.* 1986, *118*, 11.
30. Kruger, U.; Sean-Bilfinger, E.; Sturm, E.; Figala, V., Klemm, K.; Kohl, B.; Rainer, G.; Schaefer, H.; Blake, T.J.; Darkin, D.W.; Ife, R.J.; Leach, C.A.; Mitchell, R.C.; Pepper, E.S.; Salter, C.J.; Viney, N.J. *J. Chem. Org.* 1990, *55*, 4163.
31. Sean-Bilfinger, E.; Kruger, U.; Sturm, E.; Figala, V.; Klemm, K.; Kohl, B.; Rainer, G.; Schaefer, H. *J. Chem. Org.* 1987, *52*, 4582.
32. Arias, M.J.; Muñoz, P.; Moyano, J.R.; Ginés, J.M.; Novak, Cs. *J. Therm. Anal.* 1998, *51*, 973.
33. Arias, M.J.; Moyano, J.R.; Muñoz, P.; Ginés, J.M.; Justo, A.; Giordano, F. *Drug Dev. Ind. Pharm.* 2000, *26*, 253.
34. Moyano, J.R.; Arias, M.J.; Ginés, J.M.; Ortiz, M.C.; Mor, M.; Rivara, S.; Plazzi, P.V.; Giordano, F. Molecular Modelling Studies on the Interaction between Omeprazole and β-Cyclodextrin. XIV Convegno Nazionale, Divisione di Chimica Farmaceutica, Società Chimica Italiana, Salsomaggiore Terme – Parma (Italia), September 21-25 th, 1998, 151.
35. Bettinetti, G.P.; Mura, P.; Liguori, A.; Bramanti, G.; Giordano, F. *Il Farmaco* 1989, *44*, 195.
36. Lin, S.Y.; Kao, Y.H.; Yang, J.C. *Drug. Dev. Ind. Pharm.* 1988, *14*, 99.
37. Arias, M.J.; Muñoz, P.; Moyano, J.R.; Ginés, J.M.; Novak, Cs. *Int. J. Pharm.* 1996, *143*, 113.
38. Hassan, M.A.; Suleiman, M.S. and Najib, N.M. *Int. J. Pharm.* 1990, *58*, 19.
39. Khan K.A., *J. Pharm. Pharmacol.* 1975, *27*, 48.
40. Moyano, J.R.; Arias, M.J.; Muñoz, P.; Perez-Martinez, J.I.; Mor, M.; Rivara, S.; Giordano, F. *Unpublished results.*